EUROPEAN ORGANIZATION FOR NUCLEAR RESEARCH

CERN–PPE / 95–72
LIP / 95–03
12 May 1995

Recent results on dimuon production from the NA38 experiment

C. Lourenço[1)]

PPE Division, CERN, CH-1211 Geneva 23, Switzerland

ABSTRACT

We report on the production of intermediate and high mass muon pairs in p–A and S–U collisions, as measured by the NA38 experiment at the CERN SPS. The ratio between ψ' and J/ψ cross–sections is found to be constant in p–A interactions but decreases from p–A to S–U and as the released transverse energy, E_{T}, increases. While the p–A intermediate mass continuum is well explained by the superposition of Drell–Yan and charm contributions, the signal observed in the S–U data is larger than the linear extrapolation of the proton–nucleus results. No correlation is seen between dimuon and direct photon production.

Invited talk presented at Hirschegg '95: 'Hadrons in Nuclear Matter', Hirschegg, Austria, January 1995

[1)] On leave from LIP, Av. Elias Garcia 14, P-1000 Lisbon, Portugal

RECENT RESULTS ON DIMUON PRODUCTION FROM THE NA38 EXPERIMENT

Carlos Lourenço [1]

PPE Division, CERN, CH-1211 Geneva 23, Switzerland

ABSTRACT

We report on the production of intermediate and high mass muon pairs in p–A and S–U collisions, as measured by the NA38 experiment at the CERN SPS. The ratio between ψ' and J/ψ cross–sections is found to be constant in p–A interactions but decreases from p–A to S–U and as the released transverse energy, $E_{\rm T}$, increases. While the p–A intermediate mass continuum is well explained by the superposition of Drell–Yan and charm contributions, the signal observed in the S–U data is larger than the linear extrapolation of the proton–nucleus results. No correlation is seen between dimuon and direct photon production.

1 Introduction

The dimuon mass distributions produced by collisions of protons and sulphur ions, at 200 GeV per incident nucleon, on tungsten and uranium targets, have been measured by the NA38 experiment, at CERN.

In this paper, the dimuon mass spectra produced in p–W, p–U and S–U, above 1.5 GeV, are compared to the superposition of conventional sources: the J/ψ and ψ' resonances, decaying into muon pairs, the Drell–Yan mechanism and the contribution from the semi-leptonic decays of charmed mesons. In what follows, p–W and p–U are refered to by p–A. The ion events were tagged according to their $E_{\rm T}$ value, from peripheral to central collisions, in the hope of finding some *QGP like* behaviour in the 'high $E_{\rm T}$' sample, as opposed to the *p–A like* behaviour of the 'low $E_{\rm T}$' bin.

From the analysis of the S–U data collected in 1990, 1991 and (still preliminary) 1992, the NA38 experiment has obtained results on the dimuon mass region above the J/ψ resonance. Besides the study of the ψ' behaviour, identifying the high mass continuum with Drell–Yan dimuons provides a good baseline for the study of the intermediate mass region (IMR) continuum and a cleaner reference in the J/ψ suppression studies.

The study of the IMR continuum, where thermal production is sought for, faces some additional difficulties: it is ambiguous to disentangle two or three processes contributing to a continuum (while the resonances are prominent features of the mass spectra) and it is a region very much affected by the combinatorial background.

[1] On leave from LIP Lisbon

2 The NA38 experiment

The NA38 experiment measures the characteristics of the muon pairs produced in relativistic ion collisions. The detector (see Fig 1) is mainly composed of a dimuon spectrometer, an electromagnetic calorimeter, an active target and some beam counters. The muon spectrometer consists of a hadron absorber, an air-core toroidal magnet of hexagonal symmetry, 8 multiwire proportional chambers (MWPCs) and 4 hodoscopes of plastic scintillator slabs (of 2 ns time resolution) used to create the trigger. It measures the vector momenta of the muons produced in the target, from which the kinematical quantities defining the muon pairs are deduced. The mass res-

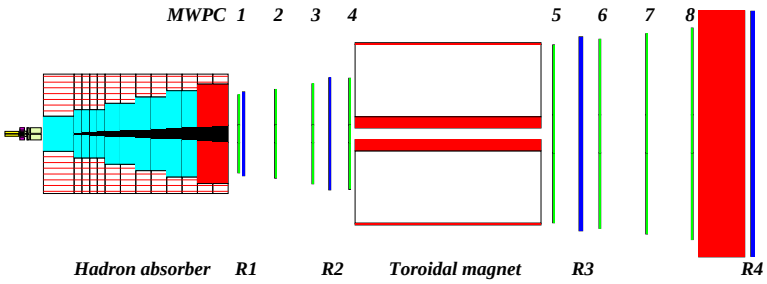

Figure 1: Overview of the NA38 detector: target region, muon filter, chambers (MWPC), hodoscopes (R), magnet, iron wall.

olution is $\sim$ 4 % (RMS) in the ψ' region. The beam dump used to stop the non-interacting beam is located far away from the target so that there is no ambiguity concerning the origin of the muon tracks, given the good vertex resolution. To cope with the rather small cross section for the production of dimuons, the experiment works close to mid rapidity, with an intense beam ($\sim 5 \times 10^7$ ions per burst) and a multiple target with 20 % of an interaction length. The dimuon characteristics were correlated with the geometry of the nucleus–nucleus collisions, on an event by event basis, via the measurement of the released transverse energy, E_{T}, performed by the electromagnetic calorimeter placed after the target box (see Fig 2). The

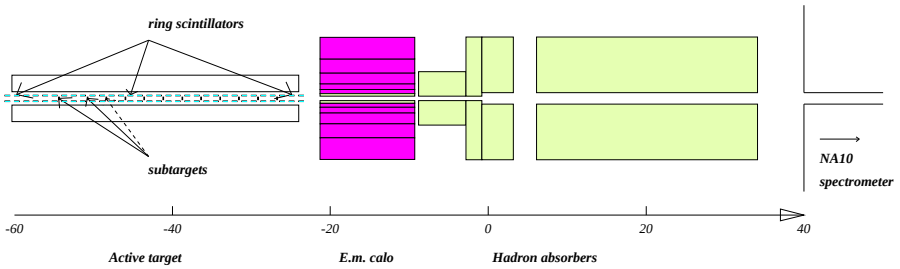

Figure 2: Overview of the target region.

multiple sub-target system identifies re-interactions of spectator fragments produced in up-stream (peripheral) collisions. Such events are rejected from the final analysis data sample. The identification of the sub-target where the interaction took place is made on the basis of the information provided by the 'target hodoscope', a set of 32 tiny cylindrical scintillators coaxial with and surrounding the targets. The high intensity of the beam imposed the choice of *quartz* Čerenkov beam counters, placed up and downstream of the target system. At such high intensities, it might happen that *two* beam particles arrive together within the calorimeter's reading time gate, Δt =20 ns. Such events are identified and tagged for (off-line) rejection, otherwise they would bias the $E_{\rm T}$ measurement.

The estimation of the combinatorial background contribution to the 'opposite-sign' muon pair mass spectra depends on the (also measured) 'like-sign' events. To make sure that the detector has the same acceptance, A, for pairs of muons with different charge combinations, a special ('image') cut was introduced in the event selection chain. An event is only accepted if the other combinations of the muons' charge and spectrometer's magnetic field signal also fulfill the trigger requirements, ensuring that $A^{+-} = A^{++} = A^{--}$.

3 Expected processes

Apart from the π/K decay background, we have assumed that the J/ψ and ψ' production, the Drell–Yan mechanism and the semi-leptonic decays of $D/\bar{D}$ mesons, are the only (signal) processes that give a significant contribution to the mass spectra above 1.5 GeV. These four processes have been simulated for each of the experimental setups considered in this work.

For the generation of J/ψ events we have used a gaussian rapidity distribution, with σ = 0.6, and a uniform cos(θ). The $M_{\rm T}$ was generated as $\mathrm{K}_1(M_{\rm T}/T)$, where K_1 is the modified Bessel function and T=195 MeV for p–A and 236 MeV for S–U. These values were tuned in successive iteractions until they provided a good reproduction of the y and $p_{\rm T}$ distributions of the events measured with mass between 2.7 and 3.5 GeV. The ψ' events were generated with the same functions except for the different mass value.

We have used PYTHIA (version 5.6) [1], as the event generator for the Drell–Yan and charm (hard scattering) processes, using leading order matrix element calculations. The GRV LO parametrization [2], as taken from the PDFLIB package [3], was chosen for the nucleon structure functions (Q^2_{min} = 0.25 GeV^2). The D$\bar{\rm D}$ events were generated with 0.80 GeV as the width of the gaussian primordial $k_{\rm T}$ distribution (as suggested by the measurements of LEBC-EHS [4]). The mass of the charm quark was assumed to be 1.5 GeV. We have verified that the mass distributions of the muon pairs originated by the decay of D and $\bar{D}$ mesons, obtained from PYTHIA with three different m_c values (1.20, 1.35 and 1.50 GeV) and three different parametrizations

of the parton distribution functions (DO 1, MRS 1 and GRV LO), can be superimposed, within statistical fluctuations, without any visible distinction. PYTHIA is restricted to collisions of protons or neutrons. Since the valence quark composition is relevant for Drell–Yan, we have generated $p-p$, $p-n$, $n-p$ and $n-n$ collisions, in this case. For charm production, dominated by gluon fusion, this is not necessary. To go from the nucleon–nucleon Drell–Yan cross–sections to the p–A and S–U values, we have assumed a linear A-dependence, neglecting any nuclear effects on the quark distributions, since our data is placed at x values where the *quark* distribution functions don't seem to be very much affected by such effects [5]. We have compared PYTHIA's Drell–Yan 'prediction' for p–Pt collisions, at 400 GeV, in $0 < x_F < 0.4$, with the corresponding data of NA3, published as detailed tables [6]. The agreement for $4.5 < M < 8.5$ GeV is quite good, as long as PYTHIA's distribution is multiplied by a K-factor, found to be 2.1 ± 0.3.

From the Monte Carlo simulation we get the mass distributions of the four considered 'signal' processes, in the 'reconstructed' variable, as they appear in the measured mass spectra. They are then fitted by empirical functions, to smooth away statistical fluctuations. The very large sample of collected J/ψ events imposes slight adjustments to the simulated line shape. The Drell–Yan and D$\bar{\text{D}}$ components of the *measured* mass spectra were found to be well described by exponential functions in the high mass region, while for mass values below 2.5 GeV the drop in acceptance requires an attenuation factor. The acceptance of the detector was calculated for each (signal) process and each data set. Typical integrated values, for $3.0 < y < 4.0$, $|\cos(\theta)| < 0.5$, and $1.5 < M < 5.5$ GeV, are $A^{J/\psi} = 19.8\,\%$, $A^{\psi'} = 20.5\,\%$, $A^{\mathrm{DY}} = 15.0\,\%$ and $A^{D\bar{D}} = 11.9\,\%$.

The background from the uncorrelated decays of π and K mesons is an important contribution to the 'opposite sign' intermediate mass continuum, measured in heavy ion collisions (see Fig 3). It is estimated by the expression

$$\frac{\mathrm{d}N}{\mathrm{d}M}^{\mathrm{Bg}} = 2 \cdot R^{\mathrm{Bg}} \cdot \left\{ \sqrt{\left.\frac{\mathrm{d}N}{\mathrm{d}M}\right|_{\oplus}^{++} \cdot \left.\frac{\mathrm{d}N}{\mathrm{d}M}\right|_{\oplus}^{--}} + \sqrt{\left.\frac{\mathrm{d}N}{\mathrm{d}M}\right|_{\ominus}^{++} \cdot \left.\frac{\mathrm{d}N}{\mathrm{d}M}\right|_{\ominus}^{--}} \right\},$$

the subscript indicating the sign of the spectrometer's magnetic field. The four like-sign functions of the right side are previously fitted to the corresponding (measured) mass spectra. For the S–U data analysis, these fits are done in each ΔE_{T} bin. The value of R^{Bg} is expected to be larger than unity in low multiplicity events (like p–A collisions), where the probability to have a certain (small) number of positive mesons is certainly correlated to the probability to have some negative mesons. While the 'signal' processes give rise to prompt muons, basically produced at the interaction vertex, the 'background' muon pairs come from the in-flight decay of π and K mesons and are strongly affected by the materials placed between the target and the muon spectrometer. This is illustrated in the right side of figure 3, where

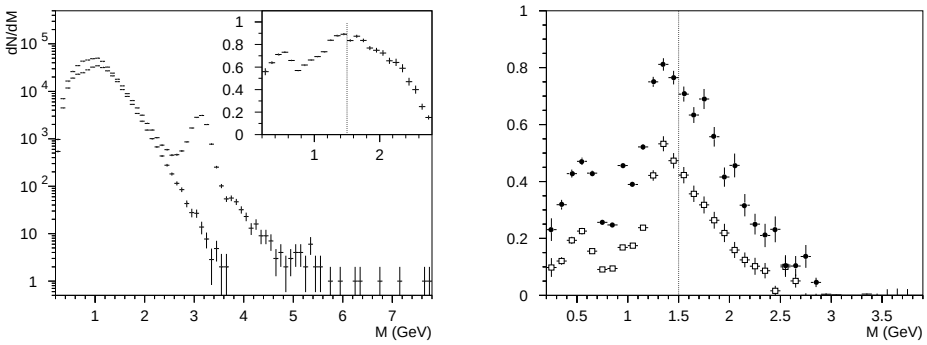

Figure 3: Left: S–U background and opposite-sign $M_{\mu\mu}$ distributions. The insert displays their ratio. Right: Same ratio for the two p–W data sets.

the ratio 'background over opposite-sign' is plotted for the two used p–W setups, very different in what concerns their hadron absorption properties. The p–A value of R^{Bg} appropriate for the NA38 experiment can be extracted by comparing the mass spectra of these two data sets. While the 'signal' cross sections must be the same, the amount of π/K decays is smaller in the setup where the hadron absorber starts closer to the target.

4 Results from the High Mass Region

While the high mass continuum is well explained by the Drell–Yan process, in the mass region below the J/ψ we also have, at least, the contribution from the semi-leptonic decay of $\mathrm{D\bar{D}}$ pairs. Since it is somewhat ambiguous to disentangle two 'continuous' contributions by means of a fit, we start by restricting the analysis to the region above 3 GeV, where the charm component can be safely neglected. The normalizations of the J/ψ, ψ' and

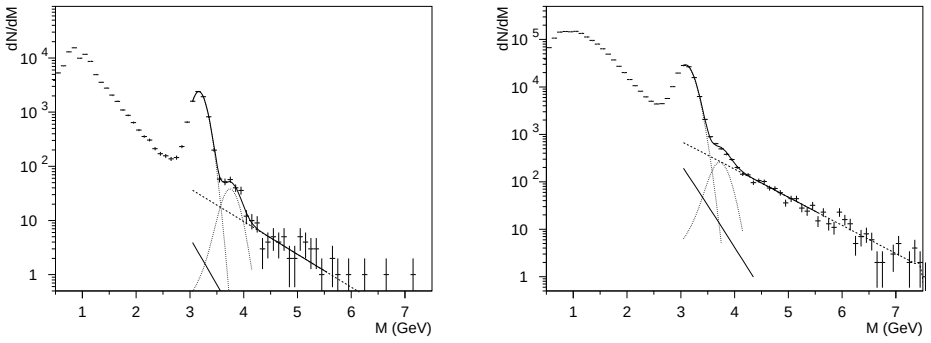

Figure 4: High mass region fits in p–W (left) and S–U (right) data.

	ψ'/ψ (%)	ψ/DY	$N^{\rm DY}$ ($\times 10^3$)	χ^2/ndf
p–W	1.80±0.17	2.55±0.25	29.5±2.9	0.80
p–U	1.77±0.22	2.76±0.38	15.5±2.1	0.95
S–U	0.93±0.08	2.03±0.09	184.1±7.8	1.12

Table 1: Results from the high mass region (HMR) fit.

Drell–Yan contributions are fitted from this region of the dimuon mass distribution (see Fig 4). The ratio ψ'/ψ (ratio of production cross-sections times branching ratios into muon pairs, since the luminosities are the same for both resonances) decreases by a factor of 2 from the values measured in p–A collisions to the value measured in S–U (see table 1). The ψ'/ψ values obtained for p–W and p–U are found to agree well with measurements of other (higher energy) experiments [7], as is shown in table 2. We have also included in this table some preliminary results concerning other NA38 / NA51 data, collected with a 450 GeV proton beam. In p–A collisions, the nuclear medium seems to treat in the same way the J/ψ and ψ' vector mesons, whatever the collision energy.

	$p_{\rm lab}$ (GeV)	$B\sigma^{\psi'}$ / $B\sigma^{\psi}$ (%)	Exp.t
p–p	$\sqrt{s} = 63$	1.9 ± 0.6	ISR
p–Li	300	1.88 ± 0.26	E 705
p–Be	400	1.7 ± 0.5	E 288
p–C	225	1.6 ± 0.9	E 444
p–C	450	2.02 ± 0.27	NA 38
p–Al	450	1.23 ± 0.35	NA 38
p–Cu	450	1.69 ± 0.14	NA 38
p–W	450	1.67 ± 0.20	NA 38
p–H_2	450	1.97 ± 0.06	NA 51
p–D_2	450	2.03 ± 0.06	NA 51

Table 2: Values of the ψ'/ψ ratio obtained with several targets and energies.

In S–U collisions, the ψ'/ψ and ψ/DY particle ratios were also obtained as a function of $E_{\rm T}$, both showing a clear tendency to decrease as $E_{\rm T}$ increases (see table 3). Since the $E_{\rm T}$ variable is quite specific of the NA38 experiment, we have computed other centrality estimators (table 4), using a simple geometrical model [8]: the mean impact parameter, b; the mean overlap area of the two nuclei, S; and the corresponding Bjorken's energy density, ϵ. The mean length the particles travel inside nuclear matter, L, is estimated assuming that the *measured* increase in the squared mean $p_{\rm T}$ value of the J/ψ is proportional to the length of nuclear medium crossed [9].

The 'charmonia suppression', as a function of $E_{\rm T}$, can be appreciated in figure 5, where the values of both ratios, ψ'/ψ and ψ/DY, are presented.

$\Delta E_{\rm T}$	ψ'/ψ (%)	ψ/DY	χ^2/ndf
10–39	1.14±0.16	2.48±0.25	1.02
39–58	1.09±0.15	2.54±0.26	1.21
58–75	0.84±0.15	1.77±0.13	1.25
> 75	0.68±0.15	1.70±0.13	0.80

Table 3: Values of the ratios ψ'/ψ and ψ/DY obtained per $\Delta E_{\rm T}$ bin.

$< E_{\rm T} >$ (GeV)	b (fm)	S (fm^2)	ϵ (GeV/fm^3)	L (fm)
24.8 (8.3)	7.03 ± 0.71	23.4 ± 5.2	1.32 ± 0.30	6.7 ± 0.8
48.7 (5.5)	5.47 ± 0.63	35.0 ± 4.5	1.74 ± 0.22	7.9 ± 0.9
66.8 (4.9)	4.06 ± 0.68	43.3 ± 2.7	1.93 ± 0.12	9.1 ± 1.1
87.4 (9.3)	2.36 ± 0.94	45.8 ± 0.4	2.39 ± 0.14	10.3 ± 1.3

Table 4: Values of several centrality estimators, alternative to $E_{\rm T}$.

The p–W points, corrected for isospin in the case of ψ/DY, are also shown to illustrate the drop from p–A to S–U. We have also included in these figures the *preliminary* values obtained from the S–U data collected in 1992.

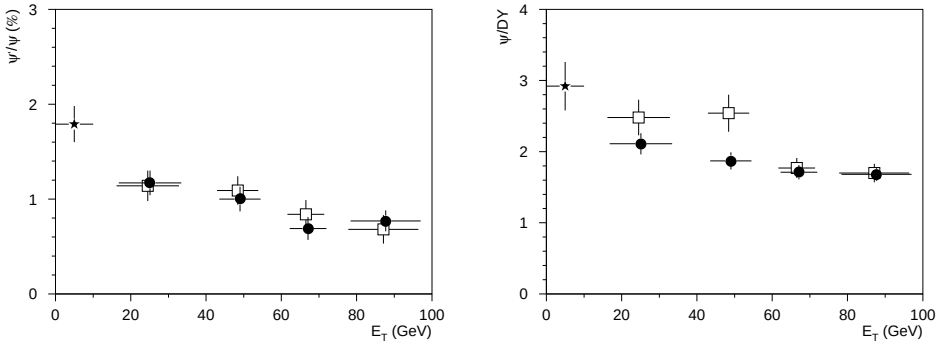

Figure 5: Ratios ψ'/ψ and ψ/DY in the 4 $\Delta E_{\rm T}$ bins of S–U. Data from 90+91 (open squares) and 92 (closed circles).

Comparing the measured Drell–Yan cross–sections with PYTHIA's predictions, we get a K-factor of 2.1 ± 0.2, both for p–W and S–U collisions, in good agreement with the measurements of previous (h–A) experiments [10]. The J/ψ and ψ' cross–sections (times their branching ratios into muons) are, respectively, 264±2 nb and 4.7±0.4 nb, in p–W, 7.78±0.04 μb and 72±6 nb, in S–U, for $3 < y_{\rm lab} < 4$ and $|\cos(\theta)| < 0.5$. The corresponding J/ψ values for $x_F > 0$ are estimated to be 564 ± 5 nb for p–W and 16.64 ± 0.08 μb for S–U, numbers in perfect agreement with those previously published by NA38 and other experiments [11].

5 Results from the Intermediate Mass Region

Using the high mass region to fix the Drell–Yan normalization, we are able to overcome the correlation between both 'continuous' signal processes in the fit to the intermediate mass region and extract the charm normalization. In the case of p–W interactions, where we have data taken with two very different setups, the charm component can be easily isolated from the combinatorial background, since (by definition) only the background can change with the geometry and properties of the absorber materials used in the experimental setup. We have (simultaneously) fitted both p–W mass distributions, between 1.5 and 2.5 GeV, leaving as free parameters the $R^{\rm Bg}$ factor and the $\rm D\bar{D}$ normalization, the other processes being determined from the high mass region. The data is well reproduced (see Fig 6) with $R^{\rm Bg} = 1.19 \pm 0.04$ and $\rm D\bar{D}/DY = 0.86 \pm 0.06$ (ratio of cross–sections in our phase space window).

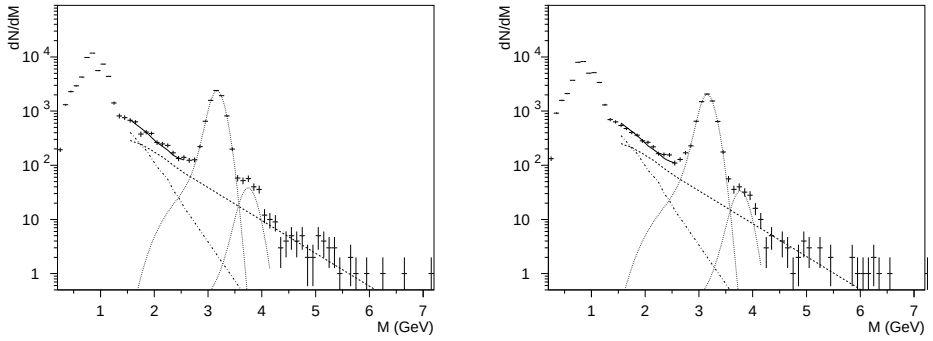

Figure 6: 'Signal' dimuon mass distributions in both p–W data sets, with the J/ψ, ψ' and Drell–Yan normalized from the HMR fit.

From the ratio $\rm D\bar{D}/DY$ and the number of Drell–Yan events we get the number of charm events (corrected for acceptances and efficiencies), which can be normalized into nb. The value obtained, 0.48 nb per target nucleon, corresponds to the cross–section for producing a pair of charmed mesons, times the probability to have both mesons decaying into muons, times the probability to have the muon pair in our phase space domain. To get a more informative quantity we have used PYTHIA to obtain the *ratio* between the total number of generated events and the number of events with a pair of muons in our kinematical window. Using this factor, 19.7×10^3, we infer the total charm production cross–section, in p–p collisions at 200 GeV, that provides the best fit to our dimuon data: 9.5 ± 2 μb. This value agrees with what we would expect, from (higher energy) direct measurements [12].

Having understood the p–A data on the basis of 'known sources' we further extrapolate into S–U interactions and compare the resulting 'expectations' with the data. To minimize the dependence on the (more uncertain)

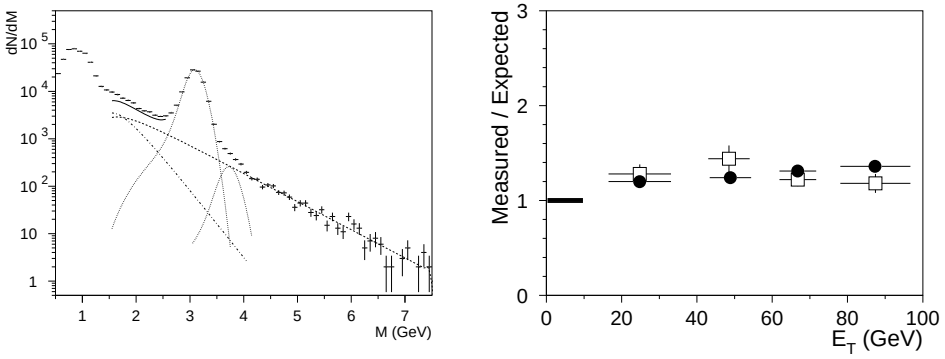

Figure 7: Left: S–U signal $M_{\mu\mu}$ distribution. Right: Ratio measured to expected signal, vs. $E_{\rm T}$, for 90+91 (squares) and 92 (circles) data.

absolute normalizations, we take from p–A the *ratio* between the $\rm D\bar{D}$ and Drell–Yan contributions to the dimuon mass spectra and assume that it remains the same in S–U collisions, apart from the Drell–Yan isospin correction. Figure 7 shows that the S–U charm contribution superposed on the (HMR) Drell–Yan line, fails to explain the intermediate mass region. We quantify the 'excess' using the ratio between the integral of the 'measured' signal mass distribution and the corresponding 'expected' value, in the mass range from 1.5 to 2.5 GeV. We observe $\sim$ 30 % more (signal) S–U events than expected from the linear extrapolation of the proton–nucleus results. Repeating this procedure per $\Delta E_{\rm T}$ bin, always using $R^{\rm Bg}$=1, we get the values presented in the right side of figure 7, the closed circles corresponding to the *preliminary* 1992 data.

6 Photons and dimuons in correlation

We now turn to the most recent result from NA38. We have used the (enhanced) ϕ and (suppressed) J/ψ mass regions to identify two event samples of (central) S–U collisions, with (maybe) different fractions of QGP events. Then we looked for another proposed signal of QGP formation, the production of direct photons, in the hope of seeing some correlation with the dimuon (anti-)signatures. While the electromagnetic calorimeter's $E_{\rm T}$ is proportional to the *neutral* multiplicity, the target hodoscope gives information on the *charged* multiplicity.

The (different) resolutions of both detectors were understood with a detailed simulation, which allowed to match the neutral and charged variables into the same (GeV) scale, as shown in the correlation plot of Fig. 8. An excess in the production of neutral particles, in the most central collisions, could be accessed through the difference $\delta \equiv E_{\rm T}^0 - E_{\rm ch}/2$, as a function of their average, $E_{\rm T}^{\rm av}$.

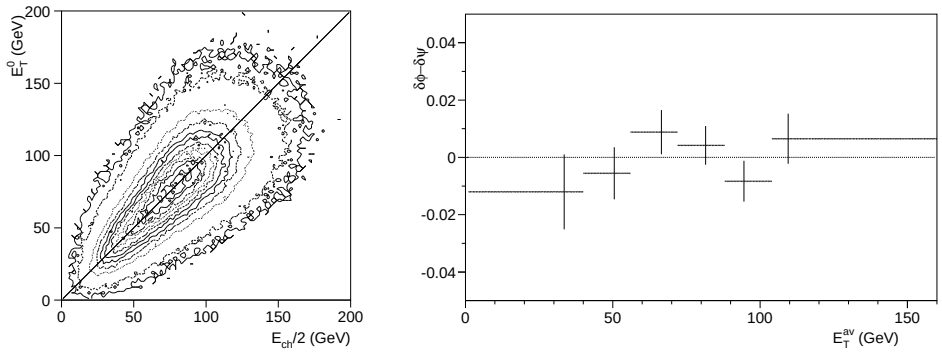

Figure 8: Left: Correlation between neutral and charged multiplicities. Right: Comparison of their difference between ϕ and J/ψ event samples.

The large ($\sim$ 25 %) systematic uncertainties cancel out when we look at the difference between the 'ϕ' and 'J/ψ' δ values, shown in the right side of figure 8. This result implies that both event samples have the same (absence of) difference between neutral and charged multiplicities, indicating that the number of direct photons eventually produced *does not increase* from the ('non-QGP') J/ψ sample to the ('QGP') ϕ sample. Integrating for $E_{\rm T}^{\rm av} > 54$ GeV (the 25 % most central collisions), and assuming the photons to be thermal, $E_{\rm T}^{0} \simeq < p_{\rm T} > \ (n_{\pi^0} + n_{\gamma})$, we derive, for the more usual γ/π^0 parameter, the relation

$$< \frac{\gamma}{\pi^0} >^{\phi} - < \frac{\gamma}{\pi^0} >^{\psi} \sim 3 \times (\delta^{\phi} - \delta^{\psi}) \sim 0.6\,(\pm 1.0)\ \% \ .$$

The absence of correlation between neutral multiplicity (excess) production and dimuon channels, accessed with good accuracy in this high statistics *multi-parameter analysis* (unusual up to now in heavy-ion physics), gives significant support to the idea that there are no direct photons being produced, in sulphur collisions, at SPS energies [13].

Summary of results

The ratio ψ'/ψ is found to be 2 times smaller in S–U than in p–A collisions. A similar 'suppression' is also seen as a function of $E_{\rm T}$, within S–U data. The absolute cross–sections measured in p–W and S–U collisions, for J/ψ and Drell–Yan production, agree well with the values previously known. While the p–A IMR *can* be understood on the basis of Drell–Yan and decays of charmed mesons, some enhancement is seen in S–U collisions, relative to the linear extrapolation of the p–A results. At the 1 % level accuracy, no correlation is seen between an eventual neutral multiplicity excess and dimuon production.

References

[1] T. Sjöstrand, Comp. Phys. Comm. **82** (1994) 74.
[2] M. Glück, E. Reya, A. Vogt, Z. Phys. **C53** (1992) 127.
[3] H. Plothow-Besch, Comp. Phys. Comm. **75** (1993) 396.
[4] M. Aguillar-Benitez *et al.,* Z. Phys. **C40** (1988) 321.
[5] D.M. Alde *et al.* (E772 Coll.), Phys. Rev. Lett. **64** (1990) 2479.
[6] J. Badier *et al.* (NA3 Coll.), Z. Phys. **C26** (1984) 489.
[7] H.D. Snyder *et al.* (E288 Coll.), Phys. Rev. Lett. **36** (1976) 1415.
A.G. Clark *et al.*, Nucl. Phys. **B142** (1978) 29.
K.J. Anderson *et al.* (E444 Coll.), Phys. Rev. Lett. **42** (1979) 944.
L. Antoniazzi *et al.* (E705 Coll.), Phys. Rev. **D46** (1992) 4828.
[8] C. Baglin *et al.* (NA38 Coll.), Phys. Lett. **B251** (1990) 472.
[9] C. Gerschel and J. Hüfner, Z. Phys. **C56** (1992) 171.
C. Baglin *et al.* (NA38 Coll.), Phys. Lett. **B268** (1991) 453.
[10] C. Grosso-Pilcher *et al.*, Ann. Rev. Nucl. Part. Sci. **36** (1986) 1.
[11] C. Baglin *et al.* (NA38 Coll.), Phys. Lett. **B270** (1991) 105.
G. Schuler, CERN-TH.7170/94 (submitted to Phys. Rep.).
[12] J. Appel, Ann. Rev. Nucl. Part. Sci. **42** (1992) 367.
[13] A. Drees, this workshop; R. Baur *et al.* (CERES/NA45 Coll.), "Search for direct photons from S–Au collisions at 200 GeV/u", in preparation.